Cell Reports
Article

Cell
PRESS

Open
ACCESS

The Mef2 Transcription Network Is Disrupted in Myotonic Dystrophy Heart Tissue, Dramatically Altering miRNA and mRNA Expression

Auinash Kalsotra,[1,6] Ravi K. Singh,[1] Priyatansh Gurha,[2,7] Amanda J. Ward,[1,3,8] Chad J. Creighton,[4] and Thomas A. Cooper[1,3,5,*]

[1]Department of Pathology and Immunology, Baylor College of Medicine, Houston, TX 77030, USA
[2]Department of Human and Molecular Genetics, Baylor College of Medicine, Houston, TX 77030, USA
[3]Department of Molecular and Cellular Biology, Baylor College of Medicine, Houston, TX 77030, USA
[4]The Dan L. Duncan Cancer Center Division of Biostatistics, Baylor College of Medicine, Houston, TX 77030, USA
[5]Department of Molecular Physiology and Biophysics, Baylor College of Medicine, Houston, TX 77030, USA
[6]Present address: Departments of Biochemistry and Medical Biochemistry, University of Illinois, Urbana-Champaign, IL 61801, USA
[7]Present address: Center for Cardiovascular Genetics, Institute of Molecular Medicine, University of Texas Health Sciences Center, Houston, TX 77030, USA
[8]Present address: Isis Pharmaceuticals, Carlsbad, CA 92010, USA
*Correspondence: tcooper@bcm.edu
http://dx.doi.org/10.1016/j.celrep.2013.12.025

SUMMARY

Cardiac dysfunction is the second leading cause of death in myotonic dystrophy type 1 (DM1), primarily because of arrhythmias and cardiac conduction defects. A screen of more than 500 microRNAs (miRNAs) in a DM1 mouse model identified 54 miRNAs that were differentially expressed in heart. More than 80% exhibited downregulation toward the embryonic expression pattern and showed a DM1-specific response. A total of 20 of 22 miRNAs tested were also significantly downregulated in human DM1 heart tissue. We demonstrate that many of these miRNAs are direct MEF2 transcriptional targets, including miRNAs for which depletion is associated with arrhythmias or fibrosis. MEF2 protein is significantly reduced in both DM1 and mouse model heart samples, and exogenous MEF2C restores normal levels of MEF2 target miRNAs and mRNAs in a DM1 cardiac cell culture model. We conclude that loss of MEF2 in DM1 heart causes pathogenic features through aberrant expression of both miRNA and mRNA targets.

INTRODUCTION

Myotonic dystrophy type 1 (DM1) is an autosomal-dominant disease caused by an expanded CTG repeat in the last exon of the *dystrophia myotonica-protein kinase* (*DMPK*) gene. Pathogenesis is caused primarily by the mRNA containing expanded CUG repeats (CUG^{exp} RNA) that is expressed from the mutated allele (Wheeler and Thornton, 2007). *DMPK* is expressed in multiple tissues that are subsequently affected in the disease, but

the primary causes of mortality are muscle wasting (60%) and sudden cardiac death (25%–30%) (Groh et al., 2008; Heatwole et al., 2012; Phillips and Harper, 1997; Salehi et al., 2007). More than 80% of individuals affected with DM1 have cardiac conduction defects and arrhythmias, and a lower percentage are affected by interstitial fibrosis and dilated cardiomyopathy (Groh et al., 2008; Lazarus et al., 2002; Nazarian et al., 2010; Pelargonio et al., 2002; Phillips and Harper, 1997; Sovari et al., 2007). Although several molecular mechanisms of DM1 pathogenesis have been defined (Sicot et al., 2011; Udd and Krahe, 2012), the specific mechanisms causing electrophysiological, fibrotic, and contractility abnormalities in DM1 heart tissue are unknown.

The best-characterized effects of CUG^{exp} RNA are disrupted functions of the RNA binding proteins muscleblind-like 1 (MBNL1) and CUGBP and Elav-like family member 1 (CELF1), which regulate multiple RNA-processing events including alternative splicing, translation, mRNA stability, and mRNA intracellular localization (Lee and Cooper, 2009; Timchenko, 2013). Celf1 is downregulated during mouse postnatal heart and skeletal muscle development while Mbnl1 activity is upregulated, driving their target alternative splicing events to the adult patterns (Kalsotra et al., 2008; Lin et al., 2006). Celf1 downregulation is posttranscriptionally mediated by microRNA (miRNA)-repressed translation and protein destabilization by dephosphorylation (Kalsotra et al., 2008, 2010; Kuyumcu-Martinez et al., 2007). CUG^{exp} RNA reverses normal postnatal regulation of MBNL1 and CELF1 by sequestration of MBNL1, which binds with high affinity to the CUG repeats, and stabilization of CELF1 by PKC-activated phosphorylation, resulting in a 2- to 4-fold increase in heart and skeletal muscle (Kuyumcu-Martinez et al., 2007; Savkur et al., 2001; Timchenko et al., 2001; Wang et al., 2007). In addition to disrupted alternative splicing, molecular defects of CUG^{exp} RNA toxicity involve repeat-associated

non-ATG (RAN) translation (Zu et al., 2011), abnormal DNA methylation (López Castel et al., 2011), bidirectional transcription (Moseley et al., 2006), and miRNA dysregulation (Fernandez-Costa et al., 2013; Perbellini et al., 2011; Rau et al., 2011).

We previously demonstrated that postnatal downregulation of Celf1 and its paralog Celf2 in mouse heart results from a dramatic upregulation of *miR-23a* and *miR-23b* between postnatal day 2 (PN2) and PN21 (Kalsotra et al., 2008, 2010). Therefore, we wanted to determine whether altered miRNA expression in DM1 could be an additional mechanism of CELF1 upregulation. Using an established heart-specific and inducible DM1 mouse model, we found that postnatal upregulation of *miR-23a* and *miR-23b* is dramatically reversed upon induction of CUG^{exp} RNA in adult heart. Furthermore, an analysis of >500 miRNAs identified 54 that are misregulated within 72 hr of CUG^{exp} RNA induction, >80% of which represent reversal of postnatal upregulation. A total of 20 of 22 miRNAs affected in the DM1 mouse model were also downregulated in DM1 heart tissues. Pathway analysis of mRNAs and miRNAs misregulated in the DM1 mouse heart identified a loss of function of the Mef2 transcriptional network. Loss of MEF2A and MEF2C mRNA and protein expression was demonstrated in heart tissue from the DM1 mouse model and in individuals affected by DM1. In addition, 20 of 20 protein-coding genes that are demonstrated targets of MEF2 were downregulated in the DM1 mouse model. Misregulation of miRNA and mRNA MEF2 targets by CUG^{exp} RNA was rescued by MEF2C. For several of the affected miRNAs, downregulation has previously been shown to produce arrhythmias or fibrotic changes. Our results demonstrate that the MEF2 transcription network is disrupted by CUG^{exp} RNA, leading to altered expression of a large number of miRNA and mRNA targets with effects consistent with DM1 heart pathology.

RESULTS

Disrupted Expression of Postnatally Regulated miRNAs in Adult DM1 Heart

To determine whether CELF1 upregulation in DM1 heart tissue resulted from altered miRNA expression, we quantified *miR-23a* and *miR-23b* expression in heart tissue from a heart-specific DM1 mouse model (EpA960; MerCreMer [MCM]). These mice inducibly express human *DMPK* exon 15 containing 960 CUG repeats and exhibit Celf1 upregulation (Figure 1A) (Wang et al., 2007). We observed a strong postnatal increase in *miR-23a* and *miR-23b* levels in wild-type mouse hearts between embryonic day 14 (E14) and adult mice as described earlier (Figure S1A) (Kalsotra et al., 2010). Importantly, the levels of *miR-23a* and *miR-23b* were significantly reduced (p < 0.05) both at 72 hr and 1 week following induction of CUG^{exp} RNA expression (Figure S1A). Comparable levels of CUG^{exp} RNA induction are observed at both time points (Figure S1B). This result identified a direct link between induction of CUG^{exp} RNA and misregulated expression of miRNAs and suggested that Celf upregulation in DM1 resulted from loss of miRNA expression in addition to the previously described phosphorylation-mediated stabilization (Kuyumcu-Martinez et al., 2007).

To determine if additional miRNAs are misregulated in DM1, we used quantitative real-time reverse-transcription PCR

(RT-PCR)-based TaqMan arrays to profile expression of >500 miRNAs from the hearts of wild-type E14 mice, adult EpA960;MCM DM1 mice, and MCM control mice. We identified 54 miRNAs that were differentially expressed (fold change > 1.8; p < 0.05) between MCM controls and DM1 mice 1 week following induction of CUG^{exp} RNA (Figure 1B; Table S1). A total of 83% (45/54) of the miRNAs are regulated during normal postnatal heart development and exhibit an adult-to-embryonic shift in expression in DM1 mice, whereas 17% (9/54) exhibit a change but are not regulated postnatally (Figure 1C). A heatmap representation of 42 miRNAs that are upregulated during normal heart development shows a striking decrease in their expression both at 72 hr and 1 week following CUG^{exp} RNA induction (Figure 1D), indicating cardiac expression of CUG^{exp} RNA results in developmental reprogramming of a subset of miRNAs.

Next, we assayed miRNA expression in heart tissues of eight DM1 and four unaffected individuals. A total of 20 out of the top 22 miRNAs found to be misregulated in the DM1 mouse model were significantly reduced (p < 0.05) in DM1 heart tissue (Figure 1E). We also determined that reduced levels of developmentally regulated miRNAs in DM1 are not a general response secondary to cardiomyopathy, as the same miRNA subset is not coordinately affected in two separate models of heart disease (Figure 1F and G) or among a subset of the miRNAs tested in human heart failure samples (Figure S1E). On the basis of these data, we conclude that reduced expression of developmentally regulated miRNAs is specific to DM1 rather than a general response to cardiac injury. In addition, the DM1 mouse model does not show activation of hypertrophy markers, suggesting that the response of the heart to induced CUG^{exp} RNA is distinct from a hypertrophic response (Figures S1B and S1C).

Altered miRNA Expression Induced by CUG^{exp} RNA Is Not Reproduced by Loss of Mbnl1 or Gain of Celf1

CUG^{exp} RNA disrupts the functions of the RNA binding proteins MBNL1 and CELF1 resulting in missplicing of their pre-mRNA targets (Lee and Cooper, 2009; Wheeler and Thornton, 2007). Altered expression of one miRNA, miR-1, in DM1 heart was proposed to result from disrupted pre-miRNA processing due to loss of MBNL1 activity (Rau et al., 2011). To determine whether the adult-to-embryonic shift in miRNA expression observed in DM1 is driven by misregulation of Mbnl1 or Celf1, we quantified expression of 23 miRNAs most affected in the DM1 mouse model in heart tissue from Mbnl1$^{ΔE3/ΔE3}$ mice (Kanadia et al., 2003) and a previously described heart-specific and tetracycline (tet)-inducible human CELF1 transgenic mouse line (Kalsotra et al., 2008; Koshelev et al., 2010). None of the miRNAs were misregulated in CELF1-inducible transgenic animals (Figure 2A) and only the three let-7 family members were reduced significantly (p < 0.05) in Mbnl1$^{ΔE3/ΔE3}$ mice (Figure 2C). Loss of Mbnl1 and gain of CELF1 activities were confirmed in the same RNA samples by showing altered splicing of Mbnl1 or CELF1 targets (Figures 2B and 2D).

To determine whether the expression of miRNA primary transcripts (pri-miRNA) were affected in the DM1 mouse model, we performed quantitative RT-PCR (qRT-PCR) analysis using TaqMan probes specific for the pri-miRNAs of ten downregulated
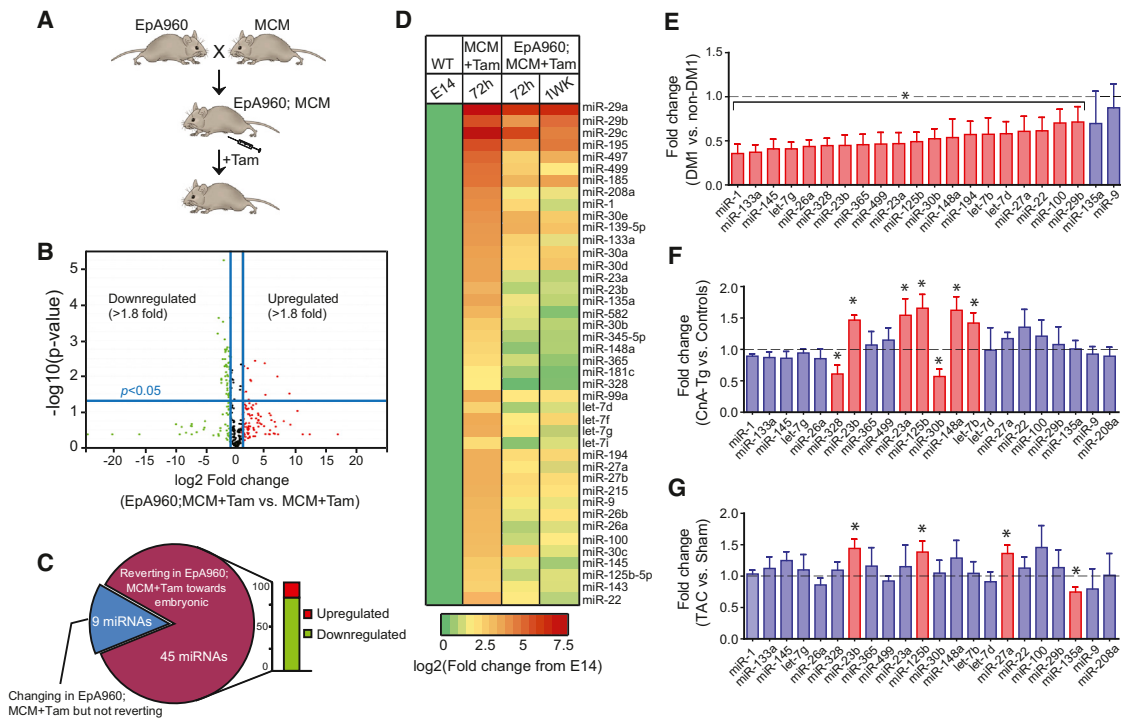
Figure 1. Misregulation of a Subset of miRNAs in a Heart-Specific Mouse Model for DM1

(A) Schematic of an inducible heart-specific DM1 mouse model. EpA960 mice contain a transgene containing *DMPK* exon 15 with 960 CTG interrupted repeats that were crossed with MerCreMer (MCM) (Sohal et al., 2001) mice to generate heart-specific and tamoxifen-inducible expression of CUG^{exp} RNA.

(B) Expression profiling using quantitative real-time RT-PCR-based TaqMan arrays of >500 miRNAs in EpA960;MCM versus MCM control mouse heart 1 week after tamoxifen injection. The volcano plot shows up- or downregulated miRNAs in DM1 mice compared to MCM controls. Data are normalized relative to U6 small nuclear RNA (snRNA) (n = 3).

(C) Adult-to-embryonic shift in miRNA expression in DM1 mice upon CUG^{exp} RNA expression. Pie chart summarizing miRNAs that are differentially expressed and exhibit a developmental shift toward the embryonic pattern.

(D) Heatmap showing developmental upregulation of 42 miRNAs during normal mouse heart development, which are downregulated at 72 hr and 1week after repeat RNA expression.

(E) Reduced miRNA expression in DM1 heart tissue. Each bar represents fold change in individual miRNA expression (mean ± SD) from heart samples of adults with DM1 (n = 8) relative to heart samples from unaffected individuals (n = 4).

(F and G) Developmentally regulated miRNAs do not show a coordinate reduction in expression in two distinct models of heart disease: calcineurin transgenic (CnA-Tg) mice (F) and wild-type mice (G) 8 weeks after transverse aortic constriction (TAC). Each bar represents fold change in individual miRNA expression (mean ± SD) from heart samples of CnA-Tg mice relative to littermate controls (n = 3) or from mice that underwent TAC surgery relative to shams (n = 3).

*p < 0.05.

miRNAs. We found that ten out of ten primary miRNA transcripts examined showed decreased expression that paralleled the reduced expression of their mature miRNAs when assayed at 72 hr and 1 week after CUG^{exp} RNA induction (Figure 2E). Moreover, we found that expression of *pri-miR-1-1* and *pri-miR-1-2* are significantly reduced in the hearts of DM1 patients relative to unaffected controls (Figure 2F). Overall, these data demonstrate that gain of Celf1 or loss of Mbnl1 activity is not responsible for the altered miRNA expression in DM1. Our data are consistent with an upstream defect in transcription rather than a downstream RNA processing defect.

Large-Scale Shift in Gene Expression in DM1 Is Partly due to Loss of miRNAs and Inactivation of the Mef2 Transcriptional Program

To assess if in addition to splicing and miRNA defects, CUG^{exp} RNA also perturbed mRNA steady-state levels, we carried out a microarray study on heart RNA from wild-type E14 and adult mice as well as adult MCM control and DM1 mice. As anticipated, we noted a large number of genes to be developmentally regulated in wild-type hearts; however, within 72 hr of CUG^{exp} RNA induction, many genes showed a coordinated adult-to-embryonic shift in mRNA expression (Figure 3A). Strikingly, 1 week of CUG^{exp} RNA expression resulted in a pervasive shift in transcript levels of a large number of genes toward the embryonic pattern (Figure 3A).

Gene Ontology analysis using the Ingenuity Pathway Analysis (IPA) showed the mitochondrial pathway as the most significantly affected pathway (p = 5.36 × 10^{-8} and threshold ratio = 0.259) (Figure S2). To identify the transcription factors and miRNAs that are potentially responsible for these gene expression changes and the ensuing phenotype in DM1 mice, we performed an upstream regulator analysis by IPA. This analysis examined the enrichment of known targets of each
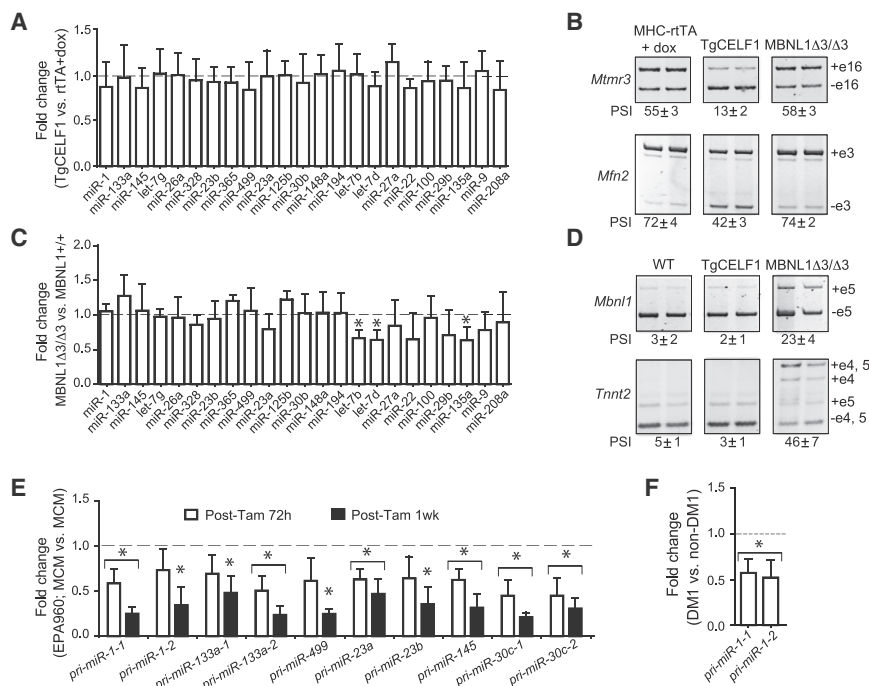
Figure 2. Altered miRNA Expression Identified in DM1 Is Not Reproduced by Loss of Mbnl1 or Gain of CELF1

(A) qRT-PCR analysis of miRNA expression in hearts of tet-inducible and heart-specific CELF1 transgenic (TgCELF1) mice. Each bar represents fold change in individual miRNA expression (mean ± SD) in TgCELF1 mice relative to MHC-rtTA controls given doxycycline (dox). Data are normalized relative to U6 snRNA (n = 3).

(B) RT-PCR analysis monitoring percent spliced in (PSI) of two CELF1-regulated alternative splicing events, Mtmr3 exon 16 and Mfn2 exon 3 in MHCrtTA or TgCELF1 mice given dox or Mbnl1$^{\Delta E3/\Delta E3}$ mice.

(C) miRNA expression in hearts of Mbnl1$^{\Delta E3/\Delta E3}$ relative to Mbnl1$^{+/+}$ mice showing fold change in individual miRNA expression (mean ± SD). Data are normalized relative to U6 snRNA (n = 3).

(D) Real-time PCR analysis monitoring PSI of two Mbnl1-regulated alternative splicing events, Mbnl1 exon 5 and Tnnt2 exon 5 in Mbnl1$^{+/+}$, TgCELF1 + dox, or Mbnl1$^{\Delta E3/\Delta E3}$ mice.

(E) Reduced expression of ten primary (pri-) miRNA transcripts at 72 hr and 1 week after CUG^{exp} RNA induction in DM1 mice. Each bar represents fold change in individual pri-miRNAs in DM1 mice relative to MCM controls at 72 hr or 1 week after tamoxifen injection.

(F) Reduced steady-state levels of pri-miR-1-1 and pri-miR-1-2 transcripts in human heart samples from DM1 patients relative to unaffected individuals (n = 3).

*p < 0.05.

transcriptional regulator present in our gene list to that in the database, resulting in an estimation of an overlap p value. Based on activation or suppression of target genes (for a transcriptional regulator) compared with observed changes in gene expression, an activation Z score was assigned. Z score > 2 illustrates activation and Z score < −2 illustrates inhibition of activity. Using this approach, we discovered the cardiac transcription factors Mef2a and Mef2c as most significantly inhibited (Mef2a Z score of −2.941, p = 1.70 × 10^{-4}; Mef2c Z score of −3.017, p = 1.20 × 10^{-7}) (Figure 3B; Table S2).

IPA also predicted inhibition of miRNA families miR-29, let-7, miR-1, and miR-34a, corroborating the reciprocal upregulation of their corresponding targets (Table S2). Finally, to understand how Mef2 and the predicted miRNAs interact with one another and their targets, we made an interaction network and overlaid it with the cardiac disease function from the function and disease tools of IPA. These analyses showed genes involved in cardiac arrhythmia, hypertrophy, and fibrosis as overrepresented in the network (Figure 3B). Importantly, these categories correlate strongly with the phenotypic changes observed in DM1 patients and mice, including prolonged PR intervals and QRS duration, decreased contractility, dilated cardiomyopathy, hypertrophy of cardiomyocytes, and proliferation of mitochondria (Wang et al., 2007).

Quantitative real-time RT-PCR assays confirmed significant downregulation (p < 0.05) of Mef2a and Mef2c mRNAs in our DM1 mouse model (Figure 4A, top) as well as in DM1 patient samples (Figure 4A, bottom). As a control, we assessed Gata4

transcript levels, which were unchanged in both the DM1 mouse model and DM1 heart tissues. MEF2A and MEF2C mRNA levels were not affected in human heart failure samples (Figure S3D), indicating that reduced expression is not a general response to heart disease. We also found that the alternative exons in Mef2a (α and β exons) and Mef2c (γ exon) did not exhibit a significant difference in percent spliced in (PSI) values following 1 week of CUG^{exp} RNA expression when compared to MCM controls (Figure S3A). Similarly, while alternative splicing of the MEF2A β exon and MEF2C γ exon were affected in some DM1 heart samples, differences are not statistically significant (Figure S3E), indicating that downregulation rather than altered splicing is likely to have the larger impact on MEF2 activity.

Western blot analysis showed a 2-fold decrease in MEF2A protein levels in DM1 compared to unaffected hearts (Figure 4B). As expected, CELF1 protein levels were induced >2-fold in DM1 heart tissue. Importantly, Mef2a and Mef2c transcripts were unaltered in hearts of either Celf1 transgenic or Mbnl1$^{\Delta E3/\Delta E3}$ mice compared to their littermate controls (Figure S3B), suggesting reduced Mef2 expression in DM1 is unrelated to the misregulation of either RNA binding protein.

Furthermore, we tested whether high-confidence Mef2 target genes expressed in heart were altered in the DM1 mouse model. A high-confidence Mef2 target was defined as a gene that has published chromatin immunoprecipitation (ChIP) evidence of Mef2 occupancy, for which promoter analysis has implicated Mef2 as a direct transcriptional activator and/or that displays decreased transcript levels upon loss of Mef2 activity. Twenty
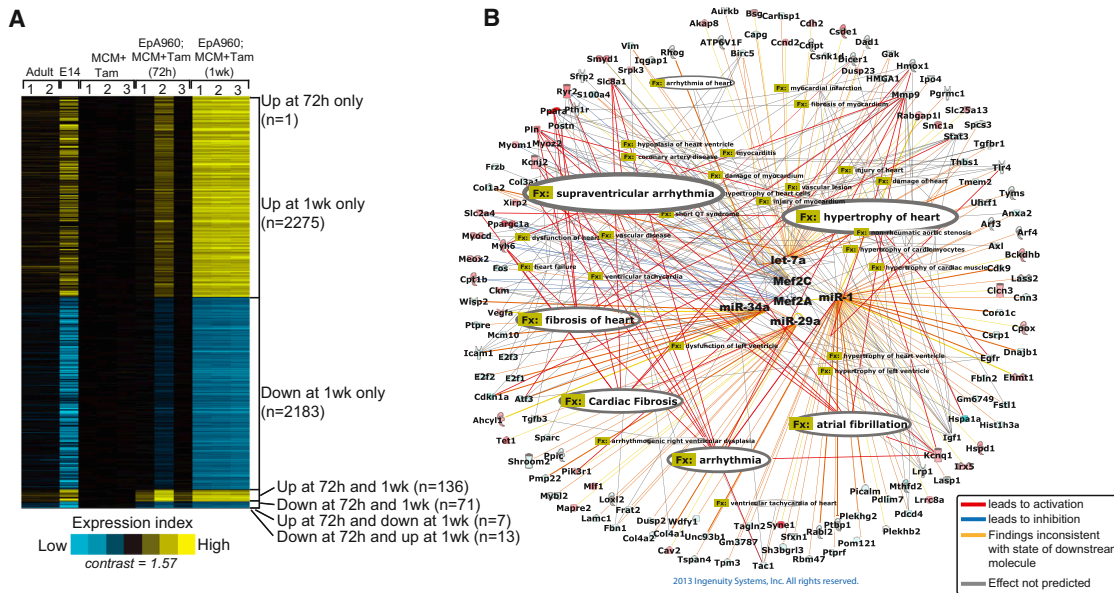
Figure 3. The DM1 Heart Mouse Model Shows a Large-Scale Shift in Gene Expression that Identifies a Disrupted Mef2 Network

(A) Gene expression profiling in mouse heart development and adult DM1 mice shows a developmental reversion in mRNA expression. Heatmap representation of transcripts overexpressed (yellow) and underexpressed (blue) in hearts of wild-type adult mice, wild-type embryonic day 14 (E14), and DM1 mice induced to express CUG[exp] RNA for 72 hr and 1week, when compared to MCM controls (p < 0.01; fold change > 1.5). Rows, transcripts (values centered on MCM group); columns, profiled samples.

(B) Ingenuity Pathway Analysis identified Mef2 as a key regulator of both miRNA and mRNA with altered expression in heart tissue expressing CUG[exp] RNA. Cardiovascular gene function categories with p < 1 × 10^{−5} are highlighted in the figure.

such targets were chosen (see the Supplemental Information). Remarkably, 100% (20/20) of the Mef2 target genes examined were downregulated in DM1 mouse heart tissue (Figure 4C, left). As a control data set, we tested a target gene set for Gata4 (see the Supplemental Information), which is unaffected in DM1 heart tissue (Figure 4A). We observed no significant change in expression of Gata4 targets in DM1 mice (Figure 4C, right). These results indicate that the vast majority of experimentally supported Mef2 target genes expressed in heart are downregulated in DM1.

## Identification of Mef2-Regulated miRNAs in Cardiac Cells

In addition to many muscle-specific genes, Mef2 directly activates transcription of bicistronic primary transcripts encoding *miR-1-2/-133a-1* and *miR-1-1/-133a-2* (Liu et al., 2007), which we found to be downregulated in DM1 patient and mouse model heart tissues. However, it is not known what other miRNAs are regulated by Mef2 in heart. We searched 10 kb genomic regions spanning each of the 54 differentially expressed miRNAs in DM1 mice for Mef2 binding sites [CTA(A/T)$_4$TAG] and found 65 putative sites in 34 different miRNA genes.

To determine the fraction of miRNA genes physically bound by Mef2 proteins in heart, we performed ChIP assays on wild-type adult mouse hearts using a pan-Mef2 antibody. Nonimmune immunoglobulin Gs (IgGs) and RNA Pol II antibodies served as negative and positive controls, respectively. The genomic regions harboring the ChIP-ed Mef2 consensus sites were amplified using specific primer sets. PCR analyses of the precipitated

chromatin showed strong Mef2 binding along the genomic regions of previously characterized Mef2 targets (*Smyd1*, *Pgc1a*, *Myom1*, and *cTnl3*), whereas no significant binding was detected to an intergenic negative control region (Figure S4A). Using the ChIP assay, we confirmed that 20 of 65 sites in 15 different pri-miRNAs were occupied by Mef2 (Figure S4B). The *let-7d* upstream region does not contain a Mef2 site and showed no binding, whereas a previously characterized *pri-miR-1-2* binding site showed positive binding, as expected. RNA Pol II showed preferential association with all miRNA and mRNA genomic regions tested, confirming these are actively transcribed in wild-type mouse hearts (Figure S4B).

To determine whether expression of the miRNAs downregulated in DM1 heart require Mef2, we used small interfering RNAs (siRNAs) to knock down *Mef2a* and *Mef2c* genes individually or in combination in mouse atrial cardiac HL-1 cells. We consistently achieved over 80% knockdown efficiency for both *Mef2a* and *Mef2c* from their endogenous levels (Figure 5A). We tested expression of three known *Mef2* target genes (*Myocd*, *Myom1*, and *Ctnna3*) in *Mef2* knockdown cultures and observed an expected reduction in their steady-state levels compared to the control knockdowns (Figure 5A). Importantly, both individual and combined *Mef2* knockdowns resulted in a significantly lower expression (p < 0.05) of 10 out of 15 *pri-miR* transcripts that showed Mef2 binding in the ChIP assays (Figure 5B; Figure S4B). A total of 4 out of 15 were not expressed in HL-1 cells, whereas pri-miR-30a was expressed but was unaffected by the knockdowns (Figure 5B). These results indicate that in addition to *pri-miR-1/-133* clusters, Mef2 proteins drive expression of
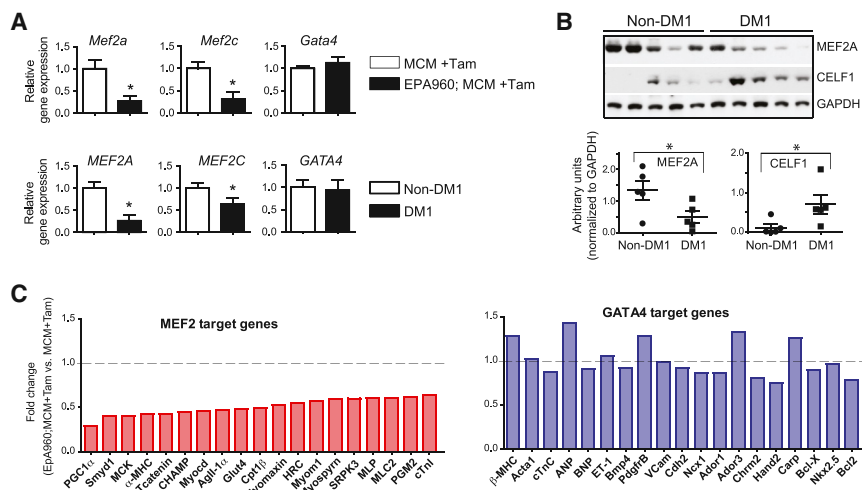
Figure 4. Disruption of the Mef2 Transcription Program in DM1

(A) Reduced *Mef2a* and *Mef2c* expression in heart tissue from the EpA960;MCM DM1 mouse model (n = 3) and individuals with DM1 (n = 8) or normal controls (n = 4). *Gata4* mRNA levels are not affected. Data are normalized to ribosomal protein L30 (*Rpl30*).

(B) Western blot showing reduction in steady-state MEF2A protein levels in human DM1 heart samples. CELF1 protein levels are upregulated in these samples, as previously described (Savkur et al., 2001; Timchenko et al., 2001). Quantification of relative band intensities, normalized to GAPDH levels, is shown below.

(C) Decreased Mef2a and Mef2c expression affects mRNA steady-state levels of Mef2 target genes in mouse DM1 heart tissue. Representative Mef2 target genes show a significant reduction in expression (light red bars), whereas Gata4 target genes are unaffected (light blue bars).

*p < 0.05.

several other *pri-miRNAs* in cardiac cells. We next used a pan Mef2 antibody to perform ChIP analysis of DM1 mouse heart tissue. Consistent with reduced Mef2a and Mef2c levels we noted their association with the response elements was decreased on both miRNA and mRNA targets in DM1 mouse heart tissues in comparison to the MCM controls (Figure 5C). Collectively, these data demonstrate that loss of Mef2 expression in DM1 is likely to have a significant impact on expression of downstream targets directly due to their reduced occupancy on the target genes.

Misregulation of miRNAs and mRNAs in a DM1 Cardiac Cell Model Is Rescued by Exogenous Mef2c

To test whether re-expression of Mef2 could rescue the loss of expression of select miRNA and mRNA targets in DM1, we infected HL-1 cells with control or tet-inducible Mef2c lentivirus that coexpresses an rtTA transactivator (Figure 6A). After a 12 hr induction of Mef2c expression with doxycycline, cells were transfected with pBi-tet-DT0-GFP or -DT960-GFP plasmids. These plasmids express GFP and the DMPK 3′ UTR with or without 960 CUG repeats through a tet-inducible bidirectional promoter (Figure 6A) (Lee et al., 2012). Thirty-six hours later, cells were either fixed for combined fluorescence in situ hybridization/ immunofluorescence analysis or lysed to extract total RNA. As shown previously (Lee et al., 2012), we found that most transfected cells that expressed GFP also formed CUG-repeat-containing RNA foci (Figure 6B). GFP expression or foci formation was not observed in the absence of doxycycline (Figures 6B and 6C), and no significant differences in DMPK mRNA levels were noted upon exogenous Mef2c expression (Figure 6C).

Similar to the DM1 mouse model and the human patient samples, transient transfection of HL-1 cells with the DT960 plasmid led to a significant decrease (p < 0.05) in endogenous *Mef2a* and *Mef2c* transcript levels when compared to the DT0 plasmid (Figure 6D). Forced expression of exogenous Mef2c in the DM1 cardiac cell model not only increased the *Mef2a* and *Mef2c* transcript levels (Figure 6D) but also rescued the expression of its mRNA and miRNA targets (Figures 6E and 6F). These results

thus provide direct evidence that misregulation of the cardiac *Mef2* regulatory network plays a fundamental role in the pathological response to CUG[exp] RNA in DM1 hearts.

DISCUSSION

We demonstrated a hierarchical relationship between expression of CUG[exp] RNA and loss of Mef2 activity using two independent experimental systems (an inducible heart-specific DM1 mouse model and a DM1 cardiac cell culture model) and validated the results in DM1 heart tissue. CUG[exp] RNA leads to an overall decrease in MEF2 expression and decreased expression of MEF2 miRNAs and mRNA targets resulting in global reprogramming of the cardiac transcriptome. Our results identify several miRNA families that are deregulated in DM1 heart tissues. This is predicted to have a cascade effect, as individual miRNAs can target multiple mRNAs (Bartel, 2009) and therefore modulate DM1 phenotype by regulating functionally related networks. For instance, *miR-1* is known to regulate gap junction proteins and cardiac channels, including Gja1, Cacna1c, and Kcnd2, and a greater than 50% reduction in its expression may directly contribute to the conduction defects seen in DM1 (Rau et al., 2011; Zhao et al., 2007). This is consistent with a previous report where genetic loss of one of the two miR-1 family members resulted in a range of cardiac abnormalities, including postnatal electrophysiological defects with a spectrum of cardiac arrhythmias (Zhao et al., 2007).

Interstitial fibrosis is another important feature of DM1 heart tissue (Nazarian et al., 2010). Our study identified dysregulation of a network of four miRNA families that may be directly responsible for this phenotype. CUG[exp] RNA expression leads to an upregulation of miR-21 and downregulation of miR-29, miR-30, and miR-133 family members. miR-21 is known to repress the Sprouty homolog 1 (3-fold downregulated in our study), a negative regulator of ERK-MAP kinase signaling, thereby leading to fibrosis (Thum et al., 2008). miR-29 represses expression of collagens (van Rooij et al., 2008), many of which are upregulated in
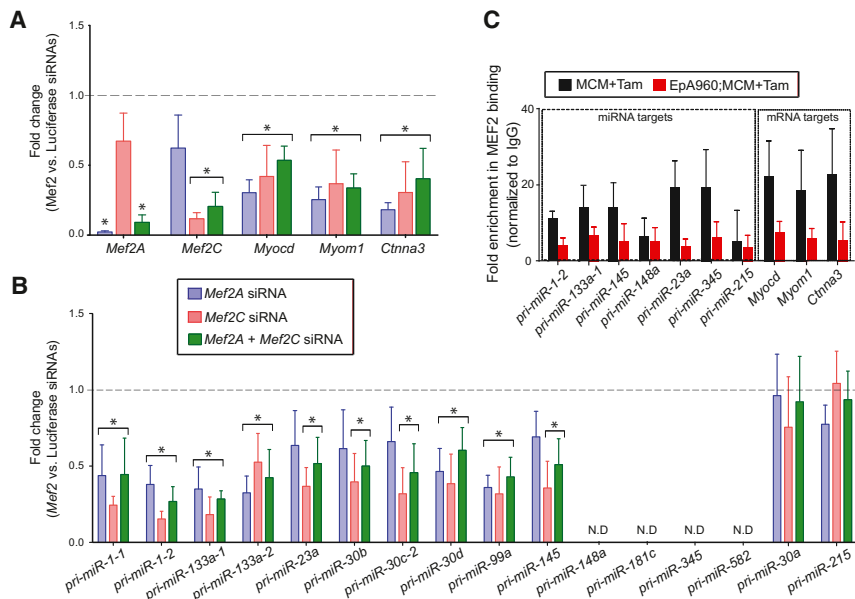
Figure 5. Identification of Mef2-Regulated miRNAs in Cardiac Cells

RNAi-based Mef2 knockdowns coupled with chromatin immunoprecipitation (ChIP) assays identify miRNAs directly regulated by Mef2.

(A) Knockdown efficiency of Mef2a and Mef2c siRNAs in HL-1 cardiac cells was determined by qRT-PCR in three independent experiments. Reduced steady-state levels of Mef2 mRNA targets Myocardin (*Myocd*), Myomesin (*Myom1*), and α-T-catenin (*Ctnna3*) in response to *Mef2A*, *Mef2C* individual or double knockdowns (mean ± SD; n = 3).

(B) Reduced steady-state levels of pri-miRNAs in *Mef2* knockdowns. All data are plotted relative to a luciferase control siRNA and expression is normalized to *Rpl30*. *p < 0.05; ND, not detected.

(C) Reduced interaction of Mef2 with its primary miRNA and mRNA gene targets in DM1 mice. Quantification of genomic DNA in chromatin immunoprecipitates using Mef2 antibody in heart tissue of MCM controls and DM1 mice. The primers used for qRT-PCR assays span the Mef2 binding sites in target primary miRNAs or mRNAs. Each bar represents mean ± SD of the fraction of input detected in the Mef2 precipitates normalized to IgG precipitates (n = 3).

our microarray study, and miR-30 and miR-133 repress expression of the connective tissue growth factor (Duisters et al., 2009), a positive regulator of fibrosis (4.8-fold upregulated in our study). Thus, the results from this study show tight reciprocal relationships between gain and loss of these four miRNAs and their target genes that support the critical role of this core network in DM1 cardiac fibrosis.

One of the clear downstream implications of miRNA dysfunction in DM1 is that reduced miR-23a/b levels lead to increased expression of its target, CELF1 protein. The miR-23a/b family regulates posttranscriptional loss of Celf1 protein during mouse postnatal heart development (Kalsotra et al., 2010). Reduced levels of both miR-23a and miR-23b in DM1 heart tissue, therefore, is expected to result in an overall increase in CELF1 protein levels, thus contributing to misregulation of CELF1 splicing targets. Together, these data indicate that dysregulation of specific miRNAs are likely to contribute to specific cardiac phenotypes observed in DM1.

MBNL1 and CELF1 are RNA binding proteins that are required for alternative splicing regulation during normal skeletal muscle and heart development (Kalsotra et al., 2008; Lin et al., 2006). Disruption of their functions by CUG[exp] RNA results in missplicing of their pre-mRNA targets such that adult tissues express embryonic splice forms. It was recently described that reduced expression of *miR-1* in DM1 patients is due in part to misprocessing of *pre-miR-1* (Rau et al., 2011). It was proposed that MBNL1 binding within the loop of *pre-miR-1* disrupts LIN28 binding to this region and thereby promotes its processing by dicer (Rau et al., 2011). Our data argue against this model, as we show that (1) primary and mature miRNAs exhibit a parallel decrease in expression in heart tissues from DM1 mouse model and patient samples and (2) Mbnl1 knockout mice do not show a significant change in miR-1 and many other miRNAs in heart. Instead, we provide evidence that a select set of miRNAs in

DM1, including miR-1, is downregulated due to a reduced MEF2 transcriptional program.

The MEF2 paralogs are a conserved family of proteins that bind to a consensus DNA sequence $CTA(A/T)_4TAG$ in the promoter region of target genes (Molkentin and Olson, 1996). Although MEF2 proteins are expressed in various tissues, the expression of the Mef2 target genes in mouse is highest in skeletal muscle, heart, and brain (Potthoff and Olson, 2007). In addition to Gata4 and Tbx5, Mef2c is a key transcription factor required for direct reprogramming of cardiac fibroblasts into induced cardiomyocytes (Ieda et al., 2010; Qian et al., 2012). This study identifies loss of Mef2 activity as causal to deregulation of many miRNAs and mRNAs in a DM1 cardiac cell culture model and heart tissue from DM1 mouse model. Reduced levels of Mef2a and Mef2c in response to transient expression of repeats in cultured cardiac cells argues for a direct effect of CUG[exp] RNA in reduction of Mef2 levels. The results we obtained in DM1 heart tissue are in contrast to results from microarray studies showing increased expression of MEF2A and MEF2C in skeletal muscle from DM1 as well as other neuromuscular disorders (Bachinski et al., 2010) and suggest different pathogenic effects of CUG[exp] RNA in heart and skeletal muscle. In summary, our data support a model in which nuclear accumulation of CUG[exp] RNA in DM1 affects a MEF2-miRNA regulatory circuit such that reduced MEF2 activity results in loss of expression of its miRNA and mRNA targets in cardiac cells. The specific mechanism by which CUG[exp] RNA affects mRNA and protein levels of MEF2 paralogs remains to be determined.

EXPERIMENTAL PROCEDURES

Animal Models and Human Tissue Samples

The tamoxifen (Tam)-inducible and heart-specific EpA960;MCM DM1 mouse model was described previously (Wang et al., 2007). CUG[exp] RNA was induced
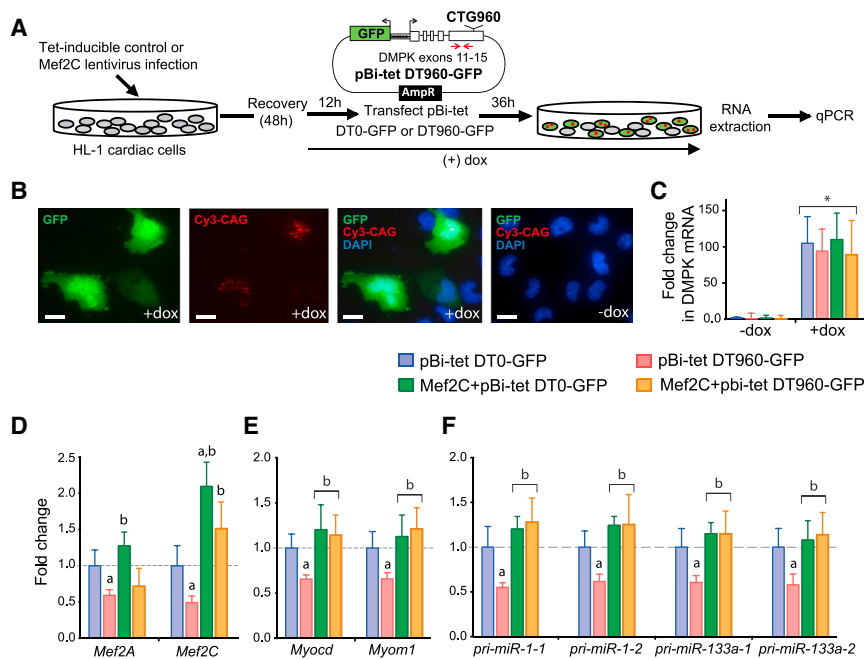
Figure 6. Rescued Expression of Mef2 miRNA and mRNAs Targets in a Cardiac Cell DM1 Model by Exogenous Mef2c

(A) Experimental schematic of Mef2c rescue in CUG^{exp} RNA-expressing cardiac cells.

(B) GFP expression was detected by indirect fluorescence using anti-GFP. RNA foci containing DT960 RNA were detected by fluorescence in situ hybridization using Cy3-labeled probes. Nuclei were counterstained with DAPI. GFP expression or RNA foci formation was not detected in the absence of dox. All images were taken at the same exposure time. Scale bars, 20 μm.

(C) Induction of DT0 and DT960 containing DMPK mRNA after dox treatment. Each bar represents fold change in expression relative to the DT0 control without dox treatment. Positions of qRT-PCR primers used to quantitate mRNA expression are indicated with red arrows. Data are normalized relative to *Rpl30*. *p < 0.05.

(D–F) Reduced (D) *Mef2A* and *Mef2C*, (E) *Myocd* and *Myom1*, and (F) *pri-miR-1-1, 1-2, 133a-1* and *133a-2* steady-state levels in response to CUG^{exp} RNA expression. Exogenous Mef2c restores the mRNA and miRNA expression in CUG^{exp} RNA-expressing cells. Each bar represents fold change in expression relative to DT0 control. a, significantly different from DT0 (infected with control virus); b, significantly different from DT960 (infected with control virus).

in 2- to 4-month-old EpA960;MCM bitransgenic animals with a single injection or five consecutive daily intraperitoneal injections of 20 mg/kg Tam (Sigma-Aldrich). Tet-inducible CELF1 bitransgenic mice (TRECUGBP1/Myh6-rtTA) were previously described (Kalsotra et al., 2008). All experiments were conducted in accordance with the National Institutes of Health *Guide for the Use and Care of Laboratory Animals* and approved by the Institutional Animal Care and Use Committee of Baylor College of Medicine. Human tissue or RNA samples were provided by Drs. C. Thornton and T. Ashizawa, X. Wehrens, National Disease Research Interchange, and the University of Miami Tissue bank. DM1 samples were from a 50-year-old male (respiratory failure [RF]), 48-year-old female (1,500 repeats, RF), 55-year-old male (pneumonia [PN]), 52-year-old female (>1,000 repeats, RF), 46-year-old male (PN), 50-year-old female (RF), 53-year-old male (unknown cause), 26-year-old male (glioma), 55-year-old male (pulmonary embolism). Normal heart samples ranged from 21- to 55-year-old pooled autopsy samples. Heart failure samples were from a 44-year-old male, 18-year-old male, and 51-year-old female.

Quantitative miRNA Profiling

TaqMan stem-loop RT-PCR MicroRNA Arrays (Applied Biosystems) were used to quantify mature miRNA expression. Briefly, 500 ng of total RNA from each sample was reverse transcribed using Megaplex RT Primers and the TaqMan miRNA reverse transcription kit. Quantitative real-time PCR reactions were performed in triplicate in a 384-well plate on a 7900HT Real-Time PCR System using ABI TaqMan Universal PCR Master Mix. An initial denaturation step of 10 min at 95°C was followed by 40 cycles of 95°C for 15 s and 60°C for 1 min. Cycle threshold (Ct) values were calculated using the SDS software v.2.3 using automatic baseline settings and a threshold of 0.2. Only the miRNAs with a Ct ≤ 35 were included in the analyses. The Ct value of an endogenous control gene (MammU6) was subtracted from the corresponding Ct value for the target gene resulting in the ΔCt value, which was used for relative quantification. Fold change of miRNA expression was calculated by the equation $2^{-\Delta\Delta Ct}$.

Microarrays

Total RNA was prepared using the RNeasy Kit (QIAGEN), and RNA quality was tested with the Agilent Bioanalyzer 2100. Total RNA was amplified and labeled using the Illumina Total Prep RNA Amplification Kit (catalog AMIL1791;

Ambion) and 500 ng of cRNA were applied to Illumina Mouse WG-6 v2 Whole-Genome Expression Beadchips. Following hybridization, washing and detection, chips were scanned using the Illumina 500GX scanner at the Genomics and Proteomics Core Laboratory at Texas Children's hospital. Expression values were quantile normalized. Genes were selected that showed differential expression between 1 week and MCM (t test p < 0.01 and fold change > 1.5) or between 72 hr and MCM; expression values were clustered as previously described (Creighton et al., 2008).

Protein and mRNA Expression Analysis

Normal (non-DM1) and DM1 human heart tissue lysates were prepared and protein concentrations were determined by BCA assays (Pierce). A total of 50 μg of lysate from each sample was separated on 10% SDS-PAGE followed by western blot. MEF2A (54 kDa; Cell Signaling Technology) CELF1 (50 kDa; 3B1), and GAPDH (36 kDa; Abcam) antibodies were used at 0.5-2 mg/mL dilution as previously described (Kalsotra et al., 2008). Anti-mouse IgG horseradish peroxidase (HRP) (Invitrogen; 1:5,000) or anti-rabbit IgG-HRP (Calbiochem; 1:10,000) were used as a secondary antibodies. After appropriate washing in PBST (0.1% Tween 20), immunoreactivity was detected by using an HRP-chemiluminescence system (Pierce). Total RNA was prepared from human heart samples using TRIzol. Steady-state mRNA expression was measured by qRT-PCR as previously described (Kalsotra et al., 2008). All individual pri-miRNA, miRNA, and mRNA qRT-PCR assays were performed using predesigned TaqMan primers and probes (Applied Biosystems) according to the manufacturer's instructions.

Alternative Splicing Assays

Total RNA (0.3–0.5 μg) was used for RT-PCR as described elsewhere (Kalsotra et al., 2010). Primer sequences for detecting alternative splicing of *Mef2a* (α and β exons) and *Mef2c* (γ exon) are provided in Table S3. PSI values for the variable region were calculated wirth Kodak Gel logic 2200 and Molecular Imaging Software as [(inclusion band)/(inclusion band + exclusion band) × 100].

Cell Culture and Transfections

HL-1 cells were cultured on gelatin (0.02%, w/v)/fibronectin (10 μg/ml) coated plates and maintained in Claycomb medium (JRH Biosciences) as previously

described (Kalsotra et al., 2010). The HL-1 cells were infected in T25 flasks with tet-inducible control or Mef2c expressing virus in presence of 5 μg/ml polybrene. After 48 hr of recovery, the cells were switched to 1 μg/ml doxycycline-containing media for 12 hr. Next, the cells were transiently transfected with pBi-tet DT0-GFP or pBi-tet DT960-GFP plasmids with Lipofectamine 2000 using the manufacturer's instructions. Cells were harvested 36 hr later in order to isolate total RNA or were fixed in 4% paraformaldehyde and permeabilized with 0.02% Triton X-100 in PBS. CUG transcripts were detected using (CAG)5-Cy3-labeled LNA probes (Exiqon) as described previously (Wang et al., 2007). Nuclei were stained with DAPI using Vectashield (Vector).

ChIP Assays

Mef2-ChIP was performed using the Imprint chromatin immunoprecipitation kit (Sigma-Aldrich) according to the manufacturer's instructions with minor modifications. Three mouse hearts each from wild-type adults, MCM mice given tamoxifen for 1 week, and DM1 mice induced to express CUG repeat RNA for a week were collected in cold PBS, chopped into smaller pieces on ice and then incubated in 1% formaldehyde in PBS for 10 min at room temperature. Formaldehyde crosslinking was stopped by adding 10X glycine to a final concentration of 1X and incubating at room temperature for 5 min. Tissue was spun at 4°C at 220 g for 5 min and the remaining tissue pellet was rinsed twice in ice-cold PBS. Tissues were harvested and lysed to isolate nuclei in a hypotonic buffer, then re-suspended, lysed in lysis buffer, and sonicated in 15 ml tubes with Bioruptor UCD-200 Diagenode (ultrasonic wave output power 250 W, 14 × 30 s) to yield chromatin size of 200–400 bp. ChIP was performed two times with 2μg of anti-RNA Pol II rabbit polyclonal (Santa Cruz Biotechnology, sc-900) and anti-pan Mef2A and Mef2C goat polyclonal (Santa Cruz, sc-313), anti-Mef2c specific rabbit polyclonal (Cell Signaling Technology, 5030) and 2μg of normal rabbit IgG (Santa Cruz, sc-2027) or goat IgG (Santa Cruz, sc-2028) as isotype controls. Coprecipitated DNA was then analyzed by qRT-PCR performed with SYBR green mix (Applied Biosystems). The primers used are listed in Table S3.

Statistics

Data are presented as mean ± SD. Statistical significance was determined with a two-tailed Student's t test or one-way ANOVA followed by post hoc Tukey's multiple range tests. A p value of less than 0.05 was considered significant.

ACCESSION NUMBERS

The NCBI Gene Expression Omnibus accession number for the microarray data reported in this paper is GSE48991.

SUPPLEMENTAL INFORMATION

Supplemental Information includes four figures and three tables and can be found with this article online at http://dx.doi.org/10.1016/j.celrep.2013.12.025.

AUTHOR CONTRIBUTIONS

A.K. designed research, performed the experiments, analyzed the data, and wrote the manuscript; R.K.S. performed experiments, analyzed data, and contributed to the manuscript; P.G. performed experiments and contributed to the manuscript; A.J.W. isolated heart tissues of EpA960;MCM animals and its controls and performed alternative splicing analysis; C.J.C. analyzed the microarray data and contributed to the manuscript; and T.A.C. supervised and designed research, analyzed the data, and wrote the manuscript.

REFERENCES

Bachinski, L.L., Sirito, M., Böhme, M., Baggerly, K.A., Udd, B., and Krahe, R. (2010). Altered MEF2 isoforms in myotonic dystrophy and other neuromuscular disorders. Muscle Nerve 42, 856–863.

Bartel, D.P. (2009). MicroRNAs: target recognition and regulatory functions. Cell 136, 215–233.

Creighton, C.J., Casa, A., Lazard, Z., Huang, S., Tsimelzon, A., Hilsenbeck, S.G., Osborne, C.K., and Lee, A.V. (2008). Insulin-like growth factor-I activates gene transcription programs strongly associated with poor breast cancer prognosis. J. Clin. Oncol. 26, 4078–4085.

Duisters, R.F., Tijsen, A.J., Schroen, B., Leenders, J.J., Lentink, V., van der Made, I., Herias, V., van Leeuwen, R.E., Schellings, M.W., Barenbrug, P., et al. (2009). miR-133 and miR-30 regulate connective tissue growth factor: implications for a role of microRNAs in myocardial matrix remodeling. Circ. Res. 104, 170–178, 6p, 178.

Fernandez-Costa, J.M., Garcia-Lopez, A., Zuñiga, S., Fernandez-Pedrosa, V., Felipo-Benavent, A., Mata, M., Jaka, O., Aiastui, A., Hernandez-Torres, F., Aguado, B., et al. (2013). Expanded CTG repeats trigger miRNA alterations in Drosophila that are conserved in myotonic dystrophy type 1 patients. Hum. Mol. Genet. 22, 704–716.

Groh, W.J., Groh, M.R., Saha, C., Kincaid, J.C., Simmons, Z., Ciafaloni, E., Pourmand, R., Otten, R.F., Bhakta, D., Nair, G.V., et al. (2008). Electrocardiographic abnormalities and sudden death in myotonic dystrophy type 1. N. Engl. J. Med. 358, 2688–2697.

Heatwole, C., Bode, R., Johnson, N., Quinn, C., Martens, W., McDermott, M.P., Rothrock, N., Thornton, C., Vickrey, B., Victorson, D., and Moxley, R., 3rd. (2012). Patient-reported impact of symptoms in myotonic dystrophy type 1 (PRISM-1). Neurology 79, 348–357.

Ieda, M., Fu, J.D., Delgado-Olguin, P., Vedantham, V., Hayashi, Y., Bruneau, B.G., and Srivastava, D. (2010). Direct reprogramming of fibroblasts into functional cardiomyocytes by defined factors. Cell 142, 375–386.

Kalsotra, A., Xiao, X., Ward, A.J., Castle, J.C., Johnson, J.M., Burge, C.B., and Cooper, T.A. (2008). A postnatal switch of CELF and MBNL proteins reprograms alternative splicing in the developing heart. Proc. Natl. Acad. Sci. USA 105, 20333–20338.

Kalsotra, A., Wang, K., Li, P.F., and Cooper, T.A. (2010). MicroRNAs coordinate an alternative splicing network during mouse postnatal heart development. Genes Dev. 24, 653–658.

Kanadia, R.N., Johnstone, K.A., Mankodi, A., Lungu, C., Thornton, C.A., Esson, D., Timmers, A.M., Hauswirth, W.W., and Swanson, M.S. (2003). A muscleblind knockout model for myotonic dystrophy. Science 302, 1978–1980.

Koshelev, M., Sarma, S., Price, R.E., Wehrens, X.H., and Cooper, T.A. (2010). Heart-specific overexpression of CUGBP1 reproduces functional and molecular abnormalities of myotonic dystrophy type 1. Hum. Mol. Genet. 19, 1066–1075.

Kuyumcu-Martinez, N.M., Wang, G.S., and Cooper, T.A. (2007). Increased steady-state levels of CUGBP1 in myotonic dystrophy 1 are due to PKC-mediated hyperphosphorylation. Mol. Cell 28, 68–78.

Lazarus, A., Varin, J., Babuty, D., Anselme, F., Coste, J., and Duboc, D. (2002). Long-term follow-up of arrhythmias in patients with myotonic dystrophy treated by pacing: a multicenter diagnostic pacemaker study. J. Am. Coll. Cardiol. *40*, 1645–1652.

Lee, J.E., and Cooper, T.A. (2009). Pathogenic mechanisms of myotonic dystrophy. Biochem. Soc. Trans. *37*, 1281–1286.

Lee, J.E., Bennett, C.F., and Cooper, T.A. (2012). RNase H-mediated degradation of toxic RNA in myotonic dystrophy type 1. Proc. Natl. Acad. Sci. USA *109*, 4221–4226.

Lin, X., Miller, J.W., Mankodi, A., Kanadia, R.N., Yuan, Y., Moxley, R.T., Swanson, M.S., and Thornton, C.A. (2006). Failure of MBNL1-dependent post-natal splicing transitions in myotonic dystrophy. Hum. Mol. Genet. *15*, 2087–2097.

Liu, N., Williams, A.H., Kim, Y., McAnally, J., Bezprozvannaya, S., Sutherland, L.B., Richardson, J.A., Bassel-Duby, R., and Olson, E.N. (2007). An intragenic MEF2-dependent enhancer directs muscle-specific expression of microRNAs 1 and 133. Proc. Natl. Acad. Sci. USA *104*, 20844–20849.

López Castel, A., Nakamori, M., Tomé, S., Chitayat, D., Gourdon, G., Thornton, C.A., and Pearson, C.E. (2011). Expanded CTG repeat demarcates a boundary for abnormal CpG methylation in myotonic dystrophy patient tissues. Hum. Mol. Genet. *20*, 1–15.

Molkentin, J.D., and Olson, E.N. (1996). Combinatorial control of muscle development by basic helix-loop-helix and MADS-box transcription factors. Proc. Natl. Acad. Sci. USA *93*, 9366–9373.

Moseley, M.L., Zu, T., Ikeda, Y., Gao, W., Mosemiller, A.K., Daughters, R.S., Chen, G., Weatherspoon, M.R., Clark, H.B., Ebner, T.J., et al. (2006). Bidirectional expression of CUG and CAG expansion transcripts and intranuclear polyglutamine inclusions in spinocerebellar ataxia type 8. Nat. Genet. *38*, 758–769.

Nazarian, S., Bluemke, D.A., Wagner, K.R., Zviman, M.M., Turkbey, E., Caffo, B.S., Shehata, M., Edwards, D., Butcher, B., Calkins, H., et al. (2010). QRS prolongation in myotonic muscular dystrophy and diffuse fibrosis on cardiac magnetic resonance. Magn. Reson. Med. *64*, 107–114.

Pelargonio, G., Dello Russo, A., Sanna, T., De Martino, G., and Bellocci, F. (2002). Myotonic dystrophy and the heart. Heart *88*, 665–670.

Perbellini, R., Greco, S., Sarra-Ferraris, G., Cardani, R., Capogrossi, M.C., Meola, G., and Martelli, F. (2011). Dysregulation and cellular mislocalization of specific miRNAs in myotonic dystrophy type 1. Neuromuscul. Disord. *21*, 81–88.

Phillips, M.F., and Harper, P.S. (1997). Cardiac disease in myotonic dystrophy. Cardiovasc. Res. *33*, 13–22.

Potthoff, M.J., and Olson, E.N. (2007). MEF2: a central regulator of diverse developmental programs. Development *134*, 4131–4140.

Qian, L., Huang, Y., Spencer, C.I., Foley, A., Vedantham, V., Liu, L., Conway, S.J., Fu, J.D., and Srivastava, D. (2012). In vivo reprogramming of murine cardiac fibroblasts into induced cardiomyocytes. Nature *485*, 593–598.

Rau, F., Freyermuth, F., Fugier, C., Villemin, J.P., Fischer, M.C., Jost, B., Dembele, D., Gourdon, G., Nicole, A., Duboc, D., et al. (2011). Misregulation of miR-1 processing is associated with heart defects in myotonic dystrophy. Nat. Struct. Mol. Biol. *18*, 840–845.

Salehi, L.B., Bonifazi, E., Stasio, E.D., Gennarelli, M., Botta, A., Vallo, L., Iraci, R., Massa, R., Antonini, G., Angelini, C., and Novelli, G. (2007). Risk prediction for clinical phenotype in myotonic dystrophy type 1: data from 2,650 patients. Genet. Test. *11*, 84–90.

Savkur, R.S., Philips, A.V., and Cooper, T.A. (2001). Aberrant regulation of insulin receptor alternative splicing is associated with insulin resistance in myotonic dystrophy. Nat. Genet. *29*, 40–47.

Sicot, G., Gourdon, G., and Gomes-Pereira, M. (2011). Myotonic dystrophy, when simple repeats reveal complex pathogenic entities: new findings and future challenges. Hum. Mol. Genet. *20* (R2), R116–R123.

Sohal, D.S., Nghiem, M., Crackower, M.A., Witt, S.A., Kimball, T.R., Tymitz, K.M., Penninger, J.M., and Molkentin, J.D. (2001). Temporally regulated and tissue-specific gene manipulations in the adult and embryonic heart using a tamoxifen-inducible Cre protein. Circ. Res. *89*, 20–25.

Sovari, A.A., Bodine, C.K., and Farokhi, F. (2007). Cardiovascular manifestations of myotonic dystrophy-1. Cardiol. Rev. *15*, 191–194.

Thum, T., Gross, C., Fiedler, J., Fischer, T., Kissler, S., Bussen, M., Galuppo, P., Just, S., Rottbauer, W., Frantz, S., et al. (2008). MicroRNA-21 contributes to myocardial disease by stimulating MAP kinase signalling in fibroblasts. Nature *456*, 980–984.

Timchenko, L. (2013). Molecular mechanisms of muscle atrophy in myotonic dystrophies. Int. J. Biochem. Cell Biol. *45*, 2280–2287.

Timchenko, N.A., Cai, Z.J., Welm, A.L., Reddy, S., Ashizawa, T., and Timchenko, L.T. (2001). RNA CUG repeats sequester CUGBP1 and alter protein levels and activity of CUGBP1. J. Biol. Chem. *276*, 7820–7826.

Udd, B., and Krahe, R. (2012). The myotonic dystrophies: molecular, clinical, and therapeutic challenges. Lancet Neurol. *11*, 891–905.

van Rooij, E., Sutherland, L.B., Thatcher, J.E., DiMaio, J.M., Naseem, R.H., Marshall, W.S., Hill, J.A., and Olson, E.N. (2008). Dysregulation of microRNAs after myocardial infarction reveals a role of miR-29 in cardiac fibrosis. Proc. Natl. Acad. Sci. USA *105*, 13027–13032.

Wang, G.S., Kearney, D.L., De Biasi, M., Taffet, G., and Cooper, T.A. (2007). Elevation of RNA-binding protein CUGBP1 is an early event in an inducible heart-specific mouse model of myotonic dystrophy. J. Clin. Invest. *117*, 2802–2811.

Wheeler, T.M., and Thornton, C.A. (2007). Myotonic dystrophy: RNA-mediated muscle disease. Curr. Opin. Neurol. *20*, 572–576.

Zhao, Y., Ransom, J.F., Li, A., Vedantham, V., von Drehle, M., Muth, A.N., Tsuchihashi, T., McManus, M.T., Schwartz, R.J., and Srivastava, D. (2007). Dysregulation of cardiogenesis, cardiac conduction, and cell cycle in mice lacking miRNA-1-2. Cell *129*, 303–317.

Zu, T., Gibbens, B., Doty, N.S., Gomes-Pereira, M., Huguet, A., Stone, M.D., Margolis, J., Peterson, M., Markowski, T.W., Ingram, M.A., et al. (2011). Non-ATG-initiated translation directed by microsatellite expansions. Proc. Natl. Acad. Sci. USA *108*, 260–265.